Composition-dependent properties and network structure of Ge-Se-Te chalcogenide glasses

L. Yang[a,b,c], G. J. Zhou[a,b,c], C. G. Lin[a,b,c,*]
[a]*Laboratory of Infrared Materials and Devices, The Research Institute of Advanced Technologies, Ningbo University, Ningbo 315211, China*
[b]*Key Laboratory of Photoelectric Detection Materials and Devices of Zhejiang Province, Ningbo 315211, China*
[c]*Engineering Research Center for Advanced Infrared Photoelectric Materials and Devices of Zhejiang Province, Ningbo University, Ningbo 315211, China*

$Ge_{12.5}Se_{87.5-x}Te_x$ ($0 \le x \le 45$) glasses were selected for elucidating the composition-dependent properties and network structure of Te-containing glasses. With increasing Te content (x), Vickers hardness (H_v) and glass transition temperature (T_g) initially increased and then decreased, showing a compositional threshold at x=27.5. It is found that the compositional trend of H_v and T_g is in good accordance with the structural evolution studied by Raman spectra. The results suggest that the introduction of Te leads to the evolution of the network connectivity and average bond strength of $Ge_{12.5}Se_{87.5-x}Te_x$ glass structure, which imposes an opposite impact on the structural properties (H_v and T_g). This work provides a new insight to the structure-property correlation of Ge-Se-Te, which would facilitate the understanding of the structural role of Te in ChGs.

(Received October 20, 2022; Accepted January 3, 2023)

Keywords: Chalcogenide glasses, Glass structure, Glass transition temperature, Raman spectra, Mechanical property

1. Introduction

Chalcogenide glasses (ChGs) have become increasingly attractive owing to their advantageous properties of excellent infrared (IR) transparency [1, 2], high linear and nonlinear refractive index [3], low phonon energy [4], and high photosensitivity [5, 6], which are promising for various applications including thermal imaging, phase-change memory, IR fiber and laser. In particular, because of its amorphous nature, the physiochemical properties of ChGs could be flexibly adjusted through compositional/structural modification [7, 8]. Consequently, knowledge of the relationship between glass composition, structure and properties of ChGs is important for elaborating new ChGs with superior properties, and also is one of the longstanding research topics in glass science. The compositional dependence on physical and structural properties of numerous ChG systems including Ge-S(Se), As-S(Se), Ge-Sb-S, and Ge-Ga-S [9-14] have been investigated

* Corresponding author: linchanggui@nbu.edu.cn
https://doi.org/10.15251/CL.2023.201.1

in detail. It provides new understanding of ChG structure, e.g., Boolchand Intermediate phase [15, 16] and phase diagram structural model [17], which are of great guidance significance for the R&D of novel ChGs.

However, despite Te-based ChGs are of important applications in far-IR region [8, 18, 19], the structure of Te-based bulk ChGs is not studied sufficiently. Pure telluride glasses are prone to crystallization during melt-quenching process, because of Te's strong metallic character. The introduction of Se into Te-based glass system can produce anion-mixed ChGs, which possess superior glass-forming ability while maintain excellent LWIR transmission. As early as 1967, Ge-Se-Te has been reported as new IR-transmitting ChG of good IR transmission from 2 to 18 μm and excellent glass-forming ability [20]. It thus provides a series of nice model glasses for exploring the composition-structure-property relationship of Te-containing glasses. Various experimental methods including XRD [21], Raman spectra [22], solid-state NMR [23, 24], and thermal analysis [25] have been employed to demonstrate the structure and properties of Ge-Se-Te glasses. The structural motifs of [$GeSe_4$] tetrahedra, Se/Te-mixed Ge tetrahedra, and Te-Te bonds were evidenced to play a dominant role in the corresponding glass network structure. To our knowledge, few investigation is focused on the compositional dependence of structural and physical properties of Ge-Se-Te, which would lead to realize new correlations [15, 16]. Because of the large glass-forming range, $Ge_{12.5}Se_{87.5-x}Te_x$ ($0 \leq x \leq 45$) glasses were selected here for elucidating the composition-dependent properties and network structure of Te-containing glasses. Compositional threshold in glass transition temperature (T_g), and hardness was found and correlated with the corresponding structural features, which were established by Raman spectra. This provides a new insight to the structure-property correlation of Ge-Se-Te, which would facilitate understanding of the structural role of Te in ChGs.

2. Experimental

$Ge_{12.5}Se_{87.5-x}Te_x$ ($0 \leq x \leq 45$) bulk glasses were prepared by traditional melt-quenching technique and subsequent annealing process. The obtained rod samples were cut and polished for the following characterization. The amorphous and crystalline characteristics of the Ge-Se-Te glasses were identified using X-ray diffraction (XRD, Bruker D2 Phaser, DE) and by comparing with the JCPDF cards of standard crystals. Thermal analysis was performed by differential scanning calorimeter (DSC, NETZSCH, DSC204F1) at a heating rate of 10°C/min.

Transmission spectra were obtained by PerkinElmer Lambda 950 spectrophotometer for the wavelength range from 0.5 to 2.5 μm and Nicolet 381 FTIR spectrometer from 2.5 to 25 μm, respectively. The Vickers hardness (H_v) and refractive indices (n) of the glasses was measured by a micro-indentation instrument (Hengyi MH-3) and an IR ellipsometer (IR-VASE MARK II, J.A. Woollam Co.), respectively. Elastic modulus was measured using cylindrical samples of Φ 9×9 mm by resonant ultrasound spectroscopy (Magnaflux, RU Spec). According to the Archimedes principle, the weights of glasses in air and alcohol were compared to obtain the value of density (ρ). Raman spectra were collected at room temperature by a Renishaw InVia Raman spectrometer under 785 nm excitation.

3. Results and discussion

Figure 1a presents the XRD patterns of several typical samples to determine the glass-forming range of $Ge_{12.5}Se_{87.5-x}Te_x$. The amorphous nature of $Ge_{12.5}Se_{87.5-x}Te_x$ ($0 \le x \le 45$) glasses is well evidenced by broad diffraction peaks in Fig. 1a, while the further introduction of Te would be phase-separated out. It is akin to the previously reported Ge-Se-Te glass-forming region obtained by water quenching [20, 26]. Figure 1b shows the transmission spectra of $Ge_{12.5}Se_{87.5-x}Te_x$ glasses with a thickness of 1mm. With the increasing Te, the short-wave cut-off edge of as-prepared glasses red shifts from 0.7 μm to 1.1 μm (the inset of Fig. 1b), whereas their long-wave cut-off edge remains around 18 μm (Fig. 1b). In addition, there have several IR absorption bands at 2.8, 4.6, and 6.3 μm, which are attributed to OH-, S-O, and H_2O impurities respectively [27, 28]. In particular, the maximum transmittance reduces gradually, which should be due to the Fresnel loss increased by the possible increasing refractive indices of the glassy samples.

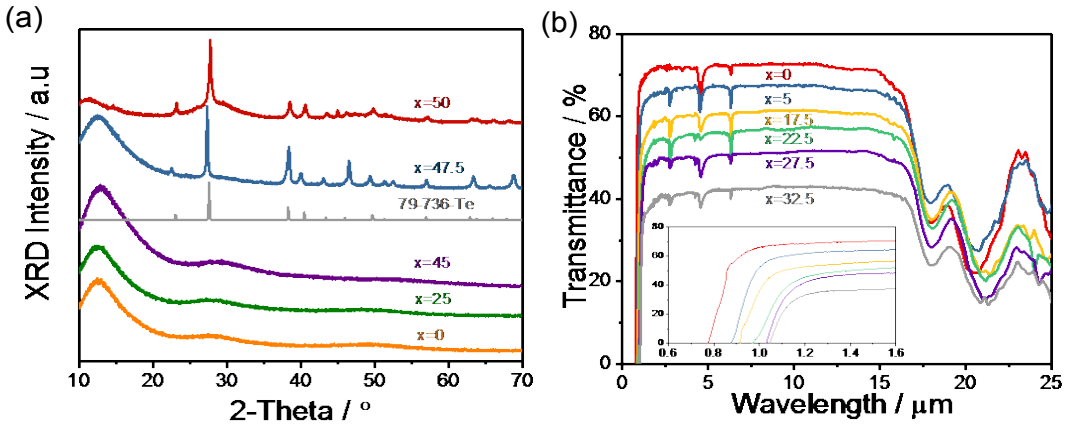

Fig. 1. (a) XRD patterns of typical $Ge_{12.5}Se_{87.5-x}Te_x$ samples (x=0, 25, 45, 47.5, and 50); (b) Transmission spectra of $Ge_{12.5}Se_{87.5-x}Te_x$ glasses.

The DSC curves of $Ge_{12.5}Se_{87.5-x}Te_x$ glasses were obtained as shown in Figure 2a. There is no crystallization peak (CP) observable for the samples with low Te content (<27.5%), indicating their relatively good thermal stability. The further introduction of Te leads to the appearance of CP, which shifts toward lower temperature with the increasing Te content. It suggests that high content of Te would weaken the thermal stability of $Ge_{12.5}Se_{87.5-x}Te_x$ glasses, and even promote the phase-separation of Te crystallites (x>45% in Fig. 1a). It is notable that the glass transition temperature (T_g) of $Ge_{12.5}Se_{87.5-x}Te_x$ glasses varies nonlinearly as a function of Te content. With the increasing Te, T_g increases gradually from 114 °C to 125 °C, and then decreases to 112°C. The corresponding T_g values were listed in Table 1, together with other physical properties including short-wave cut-off edge ($\lambda_{cut\text{-}off}$), density (ρ), refractive index at 10 μm (n_{10}), Vickers hardness (H_v), and Young's modulus (E).

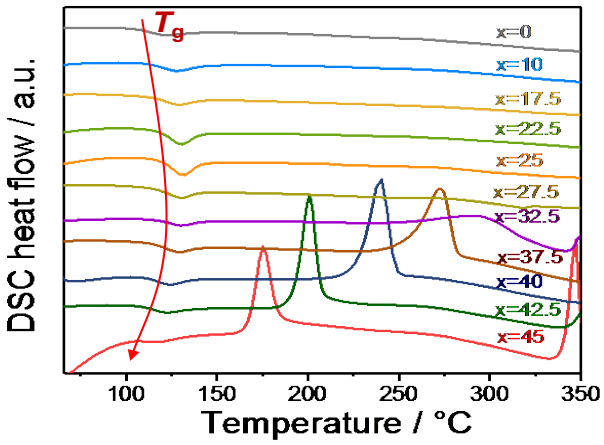

Fig. 2. DSC curves of $Ge_{12.5}Se_{87.5-x}Te_x$ glasses with a heating rate of 10 °C/min.

Table 1. The physical properties of several typical $Ge_{12.5}Se_{87.5-x}Te_x$ glasses.

x content	**$\lambda_{cut-off}$ (±1nm)**	**n_{10} (±0.001)**	**ρ (±0.002g•cm^{-3})**	**T_g (±1°C)**	**H_v (±0.02GPa)**	**E (±0.02GPa)**
0	770	2.41	4.341	114	1.06	29.033
7.5	874	2.46	4.494	118	1.08	32.563
17.5	918	2.57	4.663	120	1.10	33.129
22.5	966	2.62	4.745	123	1.16	-
32.5	1032	2.75	4.914	122	1.18	-
42.5	1048	2.85	5.037	115	1.15	43.306

Figure 3 displays the values of ρ, n_{10}, H_v, and T_g as function of Te content (x) for $Ge_{12.5}Se_{87.5-x}Te_x$ glasses. As shown in Figs. 3a and b, the ρ and n_{10} present a linear relation of Te content. Compared with selenium, Te is heavier and of larger electronic polarizabilities (Te^{2-}). Thus, the substitution of Se by Te results in the increasing of ρ from 4.341 to 5.037 g/cm^3 and n_{10} from 2.41 to 2.85, respectively. However, the T_g and H_v values present a nonlinear variation trend as a function of Te content (x) as shown in Figs. 3c and d. The H_v values here increase from 1.06 to 1.19 GPa and then decrease to 1.15 GPa (Fig. 3c). Similarly, T_g increases gradually from 114 °C to 125 °C and then decreases to 112 °C (Fig. 3d). Both indicate a compositional threshold at x=27.5. This nonlinear variation of H_v and T_g would provide new insight for understanding the correlation between properties and network structure of Ge-Se-Te ChGs, which will be discussed in the following.

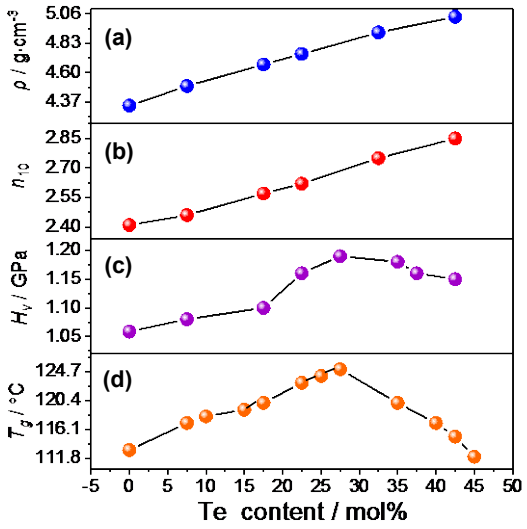

Fig. 3. The plots of (a) density (ρ), (b) refractive index at 10 μm (n_{10}), (c) Vickers hardness (H_v), and (d) glass transition temperature (T_g) as a function of Te content in $Ge_{12.5}Se_{87.5-x}Te_x$ glasses ($0 \le x \le 45$).

To explore the structural evolution of $Ge_{12.5}Se_{87.5-x}Te_x$ ($0 \le x \le 45$) glasses, their Raman spectra are collected as shown in Fig. 4. The ascription of Raman bands of Ge-Se-Te glasses has been studied in detailed previously. The main peaks at 195 and 259 cm^{-1} are attributed to the corner-sharing [$GeSe_4$] and Se-Se homopolar bonds in Se_n chains and Se_8 rings, respectively [29, 30]. And the shoulder peak at 220 cm^{-1} is ascribed to the edge-sharing [$GeSe_4$] tetrahedra. In this case, the introduction of Te into Ge-Se system leads to the formation of Te-Te and Se-Te bonds, which contribute to the appearance of Raman bands at 163 cm^{-1} and 210-217 cm^{-1}, respectively [31]. It is worthy to note that the Raman peak at 259 cm^{-1} decreases gradually as the Te content (x) increases, whereas the Raman band around 163 cm^{-1} shifts toward lower frequency and increases accordingly. The former is due to the decreasing number of Se-Se bonds; and the latter is ascribed to the formation of -$[Te]_n$- (n>3) units with the increasing Te.

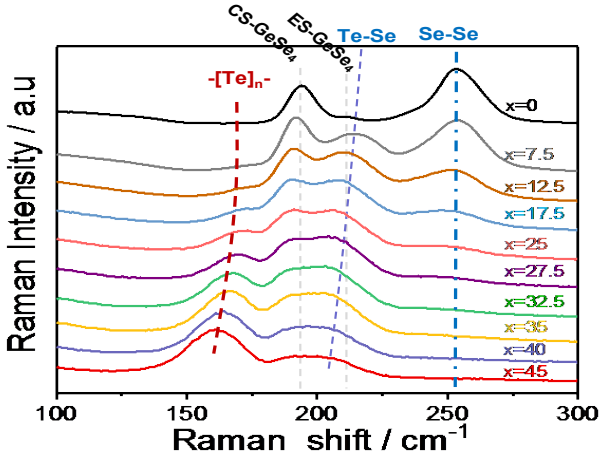

Fig. 4. Raman spectra of $Ge_{12.5}Se_{87.5-x}Te_x$ ($0 \le x \le 45$) glasses.

Figure 5 presents the variation of Raman intensity of Se-Se and Te-Te bonds, which are located at 163 cm^{-1} and 210-217 cm^{-1}, respectively, as a function of x. It is clear that the Te-Te bonds in -$[Te]_{n-}$ (n>3) units forms with the substitution of Se by Te, leading to the gradually increasing Raman intensity as shown in Fig. 5. Meanwhile, the amount of Se-Se bonds decreases, and even vanishes when x exceeds 27.5%. It is notable that the structural evolution also shows a compositional threshold at x=27.5%, which is in good accordance with that observed in H_v and T_g (Figs. 3c and d).

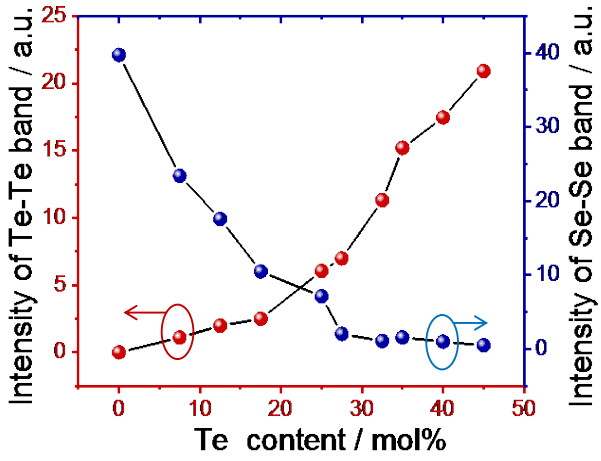

Fig. 5. The variation of Raman intensity of Se-Se and Te-Te bands as a function of Te content (x).

With the help of the compositional threshold (x=27.5), the correlation between composition, property, and structure of Ge-Se-Te glasses can be elucidated as follow. It is well known that the structural properties of H_v and T_g are generally correlated with the chemical bond strength and the cross-linking degree of glass network [32]. For the glass network possessing identical connectivity, bond strength is responsible for the compositional trends of the structural properties (H_v and T_g). As learned from Fig. 4, Ge-Se (170 kJ/mol) and Se-Se bonds (184 kJ/mol) are existed in the glass network of $Ge_{12.5}Se_{87.5}$ glass [28]. And with the introduction of Te, new bonds of Te-Se (170 kJ/mol) and Te-Te (138.2 kJ/mol) are formed in $Ge_{12.5}Se_{87.5-x}Te_x$ glasses [25, 28], at the depletion of Se-Se bonds. Consequently, the introduction of Te leads to the decreasing average bond energy of $Ge_{12.5}Se_{87.5-x}Te_x$ glasses, which should contribute to the decreasing trends of H_v and T_g. Nevertheless, it is contrary to that observed in Figs. 3c and d.

Here, the cross-linking degree of glass network should be considered to play a dominant role in these structural properties. The network structure of $Ge_{12.5}Se_{87.5}$ glass is composed of the structural motifs of Se_n chains, Se_8 rings and [$GeSe_4$] tetrahedra as shown in Fig. 4. In general, Se_8 rings do not participate in the construction of three-dimensional glass network, and strongly loose the network rigidity. With the introduction of Te, Te-Te and Te-Se structural units are formed at the consumption of Se-Se bonds in the Se_8 rings and Se_n chains. Thus, the structural connectivity of $Ge_{12.5}Se_{87.5-x}Te_x$ glasses is enhanced, with the initial increasing of Te content (x<27.5%), which is responsible for the increasing H_v and T_g as shown in Fig. 3. When *x* exceeds 27.5, as suggested in Fig. 5, there is no Se-Se bonds remained in the network structure. The further introduction of Te leads to the formation of Te-Te bonds instead of Te-Se, which decreases the average bond energy

of glass network. Consequently, the chemical bond strength plays a leading role in the decreasing trends of H_v and T_g as shown in Fig. 3. In a word, both of the chemical bond strength and the cross-linking degree of glass network contribute to the appearance of the compositional threshold at x=27.5%. In a word, both of the chemical bond strength and the cross-linking degree of glass network contribute to the appearance of the compositional threshold at x=27.5%.

4. Conclusion

The optical, thermal, and mechanical properties of $Ge_{12.5}Se_{87.5-x}Te_x$ glasses were investigated and discussed together with the structural evolution. Different from the short-wave cut-off edge ($\lambda_{cut-off}$), density (ρ), refractive index at 10 μm (n_{10}), and Young's modulus (E), the H_v and T_g values present a nonlinear compositional trend, which increasing initially and then decreasing as the introduction of Te in $Ge_{12.5}Se_{87.5-x}Te_x$ glasses. The compositional threshold of the H_v and T_g nonlinear behavior is located at x=27.5, which is in good accordance with the structural evolution studied by Raman spectra. With the introduction of Te, the formation of Se-Te and Te-Te new bonds is accompanied by the consumption of Se-Se bonds in the Se_8 rings and Se_n chains. With the increasing of Te content (x<27.5%), the initial increasing of H_v and T_g is originated from the enhanced structural connectivity of $Ge_{12.5}Se_{87.5-x}Te_x$ glasses because of the depletion of Se_8 rings and Se_n chains. When x exceeds 27.5, the chemical bond strength plays a leading role in the decreasing trends of H_v and T_g. This structural variation would lead to the changing of the network connectivity and average bond strength of glassy structure, which imposes an opposite impact on the above-mentioned properties.

Acknowledgments

This work was partially supported by the Ningbo Natural Science Foundation (Grant Nos. 20211ZDYF020195 and 202003N4008), Zhejiang Provincial Natural Science Foundation of China (Grant No. LR21E020001), and National Natural Science Foundation of China (Grant No. 62122039). It was also sponsored by K. C. Wong Magna Fund in Ningbo University.

References

[1] M. Fabian, N. Dulgheru, K. Antonova, A. Szekeres, M. Gartner. Advances in Condensed Matter Physics. 2018 (2018); https://doi.org/10.1155/2018/7158079

[2] Z. Yang,P. Lucas. Journal of the American Ceramic Society. 92(12), 2920-2923 (2009); https://doi.org/10.1111/j.1551-2916.2009.03323.x

[3] A. Seddon. Journal of Non-Crystalline Solids. 184, 44-50 (1995); https://doi.org/10.1016/0022-3093(94)00686-5

[4] D. Hewak, R. Deol, J. Wang, G. Wylangowski, J. M. Neto, B. Samson, R. Laming, W. Brocklesby, D. Payne, A. Jha. Electronics Letters. 2(29), 237-239 (1993); https://doi.org/10.1049/el:19930163

[5] V. K. Tikhomirov. Journal of Non-Crystalline Solids. 256, 328-336 (1999); https://doi.org/10.1016/S0022-3093(99)00399-3

[6] X. Wang, X. Zhao, Z. Wang, H. Guo, S. X. Gu, J. Yu, C. Liu, Q. Gong. Materials Science and Engineering: B. 110(1), 38-41(2004); https://doi.org/10.1016/j.mseb.2004.02.008

[7] F. Charpentier, B. Bureau, J. Troles, C. Boussard-Plédel, K. Michel-Le Pierres, F. Smektala, J.-L. Adam. Optical Materials. 31(3), 496-500 (2009); https://doi.org/10.1016/j.optmat.2007.10.014

[8] A. A. Wilhelm, C. Boussard-Pledel, Q. Coulombier, J. Lucas, B. Bureau, P. Lucas. Advanced Materials. 19(22), 3796-3800 (2007); https://doi.org/10.1002/adma.200700823

[9] E. Zhu, Y. Liu, X. Sun, G. Yin, Q. Jiao, S. Dai, C. Lin. Journal of Non-Crystalline Solids: X. 1, 100015 (2019); https://doi.org/10.1016/j.nocx.2019.100015

[10] S. K. Sundaram, J. S. McCloy, B. J. Riley, M. K. Murphy, H. A. Qiao, C. F. Windisch Jr, E. D. Walter, J. V. Crum, R. Golovchak, O. Shpotyuk. Journal of the American Ceramic Society. 95(3), 1048-1055 (2012).

[11] L. Petit, N. Carlie, F. Adamietz, M. Couzi, V. Rodriguez, K. Richardson. Materials Chemistry and Physics. 97(1), 64-70 (2006); https://doi.org/10.1016/j.matchemphys.2005.07.056

[12] E. Zhu, X. Zhao, J. Wang, C. Lin. Journal of Non-Crystalline Solids. 489, 45-49 (2018); https://doi.org/10.1016/j.jnoncrysol.2018.03.030

[13] D. C. Kaseman, I. Hung, Z. Gan, B. Aitken, S. Currie, S. Sen. The Journal of Physical Chemistry B. 118(8), 2284-2293 (2014); https://doi.org/10.1021/jp412451h

[14] S. Chakraborty, P. Boolchand, M. Micoulaut. Physical Review B. 96(9), 094205 (2017); https://doi.org/10.1103/PhysRevB.96.094205

[15] M. Micoulaut,J. Phillips. Journal of Non-Crystalline Solids. 353(18-21), 1732-1740 (2007); https://doi.org/10.1016/j.jnoncrysol.2007.01.078

[16] P. Boolchand, P. Chen, U. Vempati. Journal of Non-crystalline Solids. 355(37-42), 1773-1785 (2009); https://doi.org/10.1016/j.jnoncrysol.2008.11.046

[17] Z.-H. Jiang,Q.-Y. Zhang. Progress in Materials Science. 61, 144-215 (2014); https://doi.org/10.1016/j.pmatsci.2013.12.001

[18] K. Aly. Journal of non-crystalline solids. 355(28-30), 1489-1495 (2009); https://doi.org/10.1016/j.jnoncrysol.2009.05.042

[19] G. Wang, Q. Nie, X. Wang, X. Shen, F. Chen, T. Xu, S. Dai, X. Zhang. Journal of Applied Physics. 110(4), 043536 (2011); https://doi.org/10.1063/1.3626831

[20] D. J. Sarrach, J. De Neufville, W. Haworth. Journal of Non-Crystalline Solids. 22(2), 245-267 (1976); https://doi.org/10.1016/0022-3093(76)90057-0

[21] A. Moharram, M. A. Hefni, A. Abdel-Baset. Journal of Applied Physics. 108(7), 073505 (2010); https://doi.org/10.1063/1.3488907

[22] Z. Černošek, E. Černošková, M. Hejdová, J. Holubová, R. Todorov. Journal of Non-Crystalline Solids. 460, 169-177 (2017); https://doi.org/10.1016/j.jnoncrysol.2017.01.032

[23] C. Gonçalves, R. Mereau, V. Nazabal, C. Boussard-Plédel, C. Roiland, E. Furet, M. Deschamps, B. Bureau, M. Dussauze. Journal of Solid State Chemistry. 297, 122062 (2021); https://doi.org/10.1016/j.jssc.2021.122062

[24] L. B. du Bourg, C. Roiland, L. le Polles, M. Deschamps, C. Boussard-Plédel, B. Bureau, C. J.

Pickard, E. Furet. Physical Chemistry Chemical Physics. 17(43), 29020-29026 (2015); https://doi.org/10.1039/C5CP04416B

[25] S. B. Prashanth,S. Asokan. Journal of Non-crystalline Solids. 355(22-23), 1227-1230 (2009); https://doi.org/10.1016/j.jnoncrysol.2009.05.004

[26] T. Katsuyama,H. Matsumura. Journal of Applied Physics. 75(6), 2743-2748 (1994); https://doi.org/10.1063/1.356210

[27] S. Maurugeon, B. Bureau, C. Boussard-Plédel, A. Faber, X. Zhang, W. Geliesen, J. Lucas. Journal of Non-Crystalline Solids. 355(37-42), 2074-2078 (2009); https://doi.org/10.1016/j.jnoncrysol.2009.01.059

[28] L. Sun, F. Chen, Y. Xu, Y. Huang, S. Liu, Z. Zhao, X. Wang, P. Zhang, S. Dai, X. Zhang. Applied Physics A. 122(9), 1-6 (2016); https://doi.org/10.1007/s00339-016-0351-x

[29] P. Dwivedi, S. Tripathi, A. Pradhan, V. Kulkarni, S. Agarwal. Journal of Non-Crystalline Solids. 266, 924-928 (2000); https://doi.org/10.1016/S0022-3093(99)00867-4

[30] A. H. Goldan, C. Li, S. J. Pennycook, J. Schneider, A. Blom, W. Zhao. Journal of Applied Physics. 120(13), 135101 (2016); https://doi.org/10.1063/1.4962315

[31] P. Sharma,S. Katyal. Journal of Non-Crystalline Solids. 354(32), 3836-3839 (2008); https://doi.org/10.1016/j.jnoncrysol.2008.05.010

[32] J. S. Bermejo,C. M. Ugarte. Macromolecular Theory and Simulations. 18(6), 317-327 (2009); https://doi.org/10.1002/mats.200900032